Investigation of industrially relevant rheometer geometries for improved scale-up of lamellar structured liquids

Cunningham, Grace E.[1,2]; Deshpande, Shreyasi[2]; Simmons, Mark J.H.[1*]; O'Sullivan, Jonathan J.[2]

[1] Centre for Formulation Engineering, School of Chemical Engineering, University of Birmingham, Edgbaston, Birmingham, B15 2TT, UK; [2] Unilever Research & Development, Port Sunlight Laboratory, Quarry Road East, Bebington, Wirral, CH63 3JW, UK

* Corresponding author. E-mail address: M.J.Simmons@bham.ac.uk (M.J.H. Simmons)

Abstract

Lamellar gel networks (LGNs) are complex multiphase systems comprising the basis of many cosmetic and pharmaceutical formulations, owing to their stability and desirable rheology. There is comparatively little insight into the effects of processing conditions on their final rheological properties. The aim of this work is to determine the dual impact of geometry and processing conditions on mixing efficiency and resultant rheological properties of the LGN. A controlled stress rheometer with three close-clearance agitators were used to prepare LGNs under different processing conditions (temperature, speed, and time) using a fractional factorial design of experiments. Differences between the viscosity-time profiles, power requirements and aged yield stress were used to compare mixing parameters, and compared to previous work using a vane geometry. Mixing time was found to have the largest effect on yield stress (p = 0.0058), whilst 3D-ANC and 3D-HR geometries were the only ones which showed a significant difference in yield stress (p = 0.0392). The TA-HR produced homogeneous samples with the lowest power input (0.327 J/g), whereas the vane required 1.18 J/g using the same processing conditions. Overall, the study showed that to produce a homogeneous product, a viscosity peak is required before the end of the process. Moreover, a shorter mixing time following the peak viscosity produces a sample with a higher yield stress. The study expands understanding of differences in mixing profiles between geometries during manufacture of LGNs, and how processing conditions can be optimised to generate a higher yield stress system, using less energy.

Keywords: Lamellar structured liquids; Rheological mapping; Rheometer geometries; Process development; Mixing performance

1 Introduction

The global beauty and personal care market is projected to continue growing to a value of around 758 billion USD by 2025, and in order to remain competitive, businesses must reduce their time to market for new products [1]. Furthermore, with growing supply chain uncertainty due to global instabilities (*e.g.*, pandemics, global conflicts, climate change, *etc*.), it is ever more important to understand how feedstock flexibility (*i.e.*, material changes and variable quality) and process robustness could impact the formulation and properties of manufactured products [2], [3]. When a formulated product is brought to market, it is first developed at a traditional laboratory scale (<1kg), before being progressed to a pilot plant environment (5-50kg), and once the formulation and process conditions are confirmed, then deployed to factory-scale at a sourcing unit (>1,000kg). The scale of the process impacts both mixing and temperature profiles experienced by the raw materials, which affects the final product microstructure and physical properties [4]. Having a representative scaled-down version of the manufacturing process would enable improved screening of new ingredients, better understanding of the impact of process conditions on microstructure formation and aid the scale-up process by improving geometric similarity and understanding of power requirements.

Previous work by Cunningham *et al*. [5] employed a rheometer to monitor the evolution of the structure of lamellar gel networks (LGNs) as a function of process conditions such as time, agitator speed and temperature. However, one of the limitations of this work was the use of a vane geometry as the agitator. The vane geometry has gained popularity for measuring the yield stress and other rheological properties of complex fluids (*e.g.*, thixotropic, viscoelastic, plastic, *etc.*) due to its ability to inhibit slip, as the shape of the vane generates a cylindrical stress field around the rotating central axis, but the blades of the vane reduce slip compared to a cylindrical Couette geometry [6]. Whilst it is known that in practice this is not always the case, and that there can be mixing between the quadrants of the vane, it would be pertinent to utilise rheometer geometries that both promote mixing and possess geometric similarities to industrial mixing elements [7]. Therefore, the main objective of this work was to utilise bespoke rheometer geometries which

more accurately reflect the geometric considerations of agitators employed at industrial scale. The study will aim to determine any differences in viscosity profile, mixing efficiencies, power requirements and final product characteristics that arise from using different geometries to manufacture lamellar structured liquids. The application of such capabilities at a rheometer scale could enable such tools to be used for broader process understanding, minimising the number of pilot scale trials that are required, reducing material and energy consumption.

2 Materials and Methods

2.1 Materials

The fatty alcohol (FA) used as part of this study was a commercially available blend of cetyl alcohol (30 wt. %) and stearyl alcohol (70 wt. %) (cetostearyl alcohol) sourced from Godrej Industries (India). The surfactant used was behentrimonium trimethyl ammonium chloride (BTAC), supplied by Clairant International Ltd. (Germany). This surfactant is provided at 70 wt. % purity, where the remaining 30 wt. % is comprised of dipropyl glycol. Distilled water was used for all experiments.

2.2 Preparation of lamellar structured liquids

A Discovery HR-III stress controlled rheometer (TA Instruments, UK) was used to prepare the lamellar structured liquids according to the methods given in [5], with some slight differences. In this work, three, new different geometries were investigated: TA helical rotor (TA Instruments, part no. 546018.901), 3D printed helical ribbon, and 3D printed anchor scraper (Figure 1) where the 3D printing process was direct metal laser sintering of titanium conducted by Laser Prototypes Europe Ltd (UK). The geometric considerations for the bespoke mixing elements were based on representative pilot-scale examples.

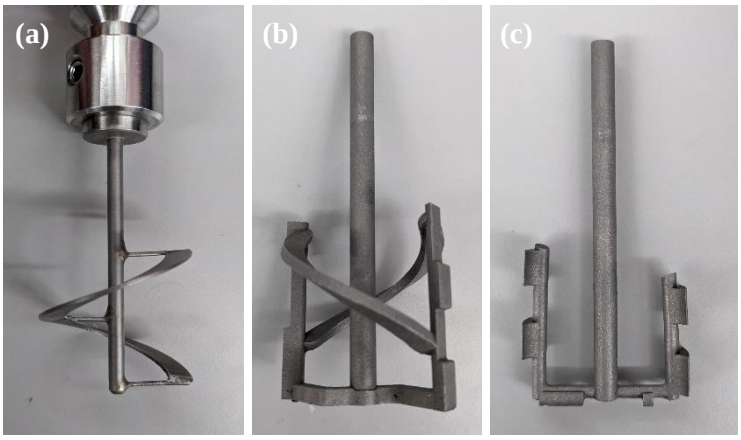

Figure 1 – (a) TA Instruments helical rotor (TA-HR), (b) 3D printed helical ribbon (3D-HR), and (c) 3D printed anchor (3D-ANC)

Similar to the previous study [5], variables were changed during the structuring stage of the process (addition of BTAC to a molten mix of FA and water). A fractional factorial design of experiments was used to investigate the effects of process temperature (T, -), agitator speed (N, rad s^{-1}) mixing time (t, min) and rheometer geometry (Table 1). Process conditions utilised in the previous study have been repeated in this work to enable direct comparison. Two temperatures from the previous work were selected for further investigation - the reference temperature, and the highest temperature (referred to in this work as T = REF, T = HIGH, respectively) [5]. Furthermore, it should be noted that angular velocity has been used to quantify agitator speed rather than shear rate, in order to directly compare differences in speed across different geometries.

Table 1. Fractional factorial design of experiments of process variables (geometry, temperature, agitator speed and time) for the structuring stage of lamellar gel formation. Sample naming system is Geometry_Temperature_Speed_Time

Sample	**Rheometer geometry**	**Temperature (-)**	**Speed (rad s^{-1})**	**Time (min)**
3D-HR_REF_48_30	3D-HR	REF	48	30
TA-HR_REF_16_30	TA-HR	REF	16	30
3D-ANC_REF_16_30	3D-ANC	REF	16	30
TA-HR_REF_48_10	TA-HR	REF	48	10
TA-HR_HIGH_48_30	TA-HR	HIGH	48	30
TA-HR_HIGH_16_10	TA-HR	HIGH	16	10
3D-ANC_HIGH_48_10	3D-ANC	HIGH	48	10
3D-ANC_REF_48_10	3D-ANC	REF	48	10
3D-HR_HIGH_48_30	3D-HR	HIGH	48	30
3D-ANC_HIGH_16_30	3D-ANC	HIGH	16	30
3D-HR_REF_16_10	3D-HR	REF	16	10
3D-HR_HIGH_16_10	3D-HR	HIGH	16	10
3D-HR_REF_16_30	3D-HR	REF	16	30

2.3 Calibration of Rheometer Geometries

The TA-HR, 3D-HR, and 3D-ANC were calibrated using the Couette analogy as recommended by the rheometer equipment supplier, TA Instruments [8], and described by Ait-Kadi *et al*. [9]. The calibration fluid was glycerine (Palmera G995E; >99.5% purity; supplied by KLK Oleo; viscosity at 0.25°C = 0.95 Pa s). The values calculated for the shear stress constant (K_τ) and the shear rate constant ($K\gamma$) are given below in Table 2.

Table 2. Summary of shear rate and shear stress constants for the different geometries investigated

Geometry	**Shear stress constant (Pa. Nm)**	**Shear rate constant (rad^{-1})**
Vane	16141	12.21
3D-ANC	23836	3.43
3D-HR	21891	4.51
TA-HR	26800	2.46

2.4 Rheological and Homogeneity Characterisation of LGN Samples

The samples were characterised by measuring rheological properties and visual assessment of homogeneity, in addition to the in-situ process data that was captured during the manufacture of the LGN samples. Rheological characterisation of all samples was carried out using the

Discovery DHR-III stress controlled rheometer (TA Instruments, UK) equipped with cross-hatched parallel plates to minimise slip effects. All measurements were carried out at 25°C on samples aged for at least 24 h. The yield stress was measured using an oscillation amplitude sweep method described in [5], [10]. A visual assessment of homogeneity was carried out by spreading *ca.* 1 g sample of LGN to a thickness of *ca.* 1 mm on to a matte black tile and observing for both lumps of unincorporated FA or BTAC, and opacity.

2.5 Statistical Analysis

All samples were manufactured in triplicate, and an average of the viscosity profile is presented in this work. In addition, yield stress measurements were completed in triplicate (individual measures on samples prepared in triplicate) and an average and standard deviation is presented. ANOVA was used to determine the difference between single effects on single outputs, where a 95% confidence interval was employed, and data was considered statistically significant when $p < 0.05$.

3 Results & Discussion

3.1 Comparison of viscosity-time profiles of industrially relevant geometries to vane geometry

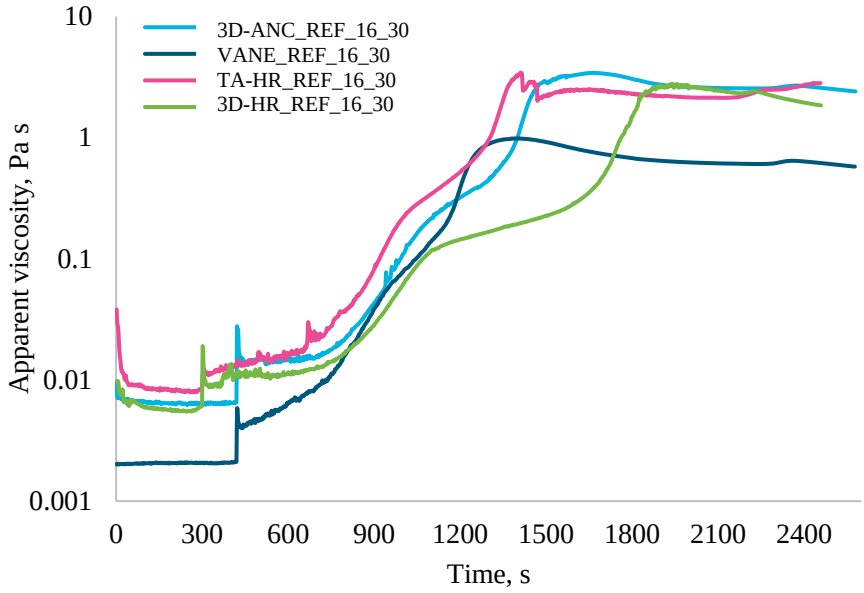

Figure 2. Viscosity profiles for samples prepared at T=REF, N = 16 rad s^{-1}, t = 30 min

The impact of different rheometer geometries (vane, 3D-ANC, TA-HR, 3D-HR) on the formation of lamellar gel structure was initially investigated at the same processing conditions of T=REF, N=16 rad s^{-1}, t= 30 min (*i.e.*, REF_16_30 according to the naming convention used).

Figure 2 shows the viscosity profiles for these samples (VANE_REF_16_30, 3D-ANC_REF_16_30, TA-HR_REF_16_30, 3D-HR_REF_16_30). In general, the viscosity profiles predominantly follow the same trend of a slow initial increase in viscosity, followed by two changes in the rate of viscosity increase, before reaching a peak value. After this point, the viscosity plateaus until the cooling stage commences, where there is another slight peak. However, the rate of viscosity increase, and the point at which the system reaches the peak viscosity varies between geometries. The relationship between viscosity and structure formation has been discussed previously by Cunningham *et al*. [5].

Whilst they generally follow the same trend, the viscosity measurements for 3D-ANC and TA-HR were significantly greater than for the vane throughout the process, where this can be

accounted for by the difference in shear rate constants for the different geometries (Table 2). The equivalent shear rate for the same speed was at least three times higher for the vane than the other investigated geometries; thus, for a shear thinning LGN system, the apparent viscosity was lower (Figure 2) [11]. However, it would be expected that the viscosity values for 3D-HR would also be similar to the 3D-ANC based on their similar shear rate constants. The viscosities start at similar values, but around 900 s, the rate of viscosity increase is much slower for the 3D-HR than the 3D-ANC, and the 3D-HR does not achieve the peak viscosity until much later than the rest of the samples (1942 s). The peak viscosities for the vane and TA-HR occur around the same time (1400 s, 1414 s, respectively), whilst the peak viscosity for 3D-ANC occurs later (1670 s). If we consider the time of peak viscosity as an indicator of mixing efficiency, the vane and TA-HR are the most efficient, followed by 3D-ANC and then 3D-HR.

For the sample prepared using the TA-HR, after the peak viscosity (t = 1414 s), there are two perturbations in the curve. This behaviour is thought to be associated with when the system became too viscous at the peak viscosity for the TA-HR to mix the fluid properly, as it was visually observed that the material started moving as a solid body in the vessel and this was seen for the other investigated process conditions with the TA-HR geometry. This issue could potentially be resolved using a serrated or roughened cup to reduce slip effects. The shear rate constant for the TA-HR is the lowest for all the geometries investigated (Table 2), which means that for the same speed, the least power is inputted into the system in comparison to the other investigated geometries. Mihailova *et al*. [12] noted a relationship between the torque and power requirements and the surface area of the agitator which is in contact with the liquid, where a larger surface area provides greater resistance to motion, and thus a higher torque response. A similar relationship between has been seen in this work, in which the TA-HR has the smallest surface area and smallest power draw, and this is reflected in the value of the shear rate constant (Table 2).

The peak viscosity value was lowest for the sample prepared with the vane (0.99 Pa s), as expected due to the difference in shear rate constants previously discussed. However, when

comparing the three industrially relevant geometries, the peak viscosity for 3D-HR (2.78 Pa s) was lower than that for 3D-ANC and TA-HR (3.43 Pa s and 3.45 Pa s, respectively). This, in addition with the longer time to achieve peak viscosity again suggests poorer mixing by the 3D-HR geometry than by the 3D-ANC and TA-HR.

Nevertheless, the yield stress of the samples discussed here, prepared at the same processing conditions, were not significantly different ($p > 0.05$; vane = 108±5 Pa; 3D-ANC = 111 Pa, TA-HR = 106 Pa, 3D-HR = 108 Pa).

The energy required to achieve the peak viscosity is similar for the vane and the 3D-ANC, but not for TA-HR (vane = 1.18 J/g, 3D-ANC = 1.18 J/g, TA-HR = 0.327 J/g). Again, this suggests that the TA-HR promotes better mixing than the anchor and the vane and is able to achieve homogeneity with a smaller power input. For the process conditions discussed above, the geometry appears to have minimal effect on the type of structure formed, or the final rheological properties of the system (yield stress), but does affect the mixing characteristics, evidenced by the difference in times to achieve peak viscosity and the inflections in the viscosity-time profile for the TA-HR, in comparison to the other investigated geometries (Figure 2).

3.2 Effect of mixing time on LGN formation

In [5], the conditions which provided the highest yield stress sample were T = REF, N =16 rad s^{-1}, t = 10 min. Thus, it was hypothesised that a shorter mixing time would also increase the yield stress for the geometries investigated in this study. Figure 3 shows the viscosity profiles for four samples prepared with a 10 minute structuring stage time and 16 rad s^{-1} agitator speed (vane and 3D-HR at T=REF, TA-HR and 3D-HR at T=HIGH).

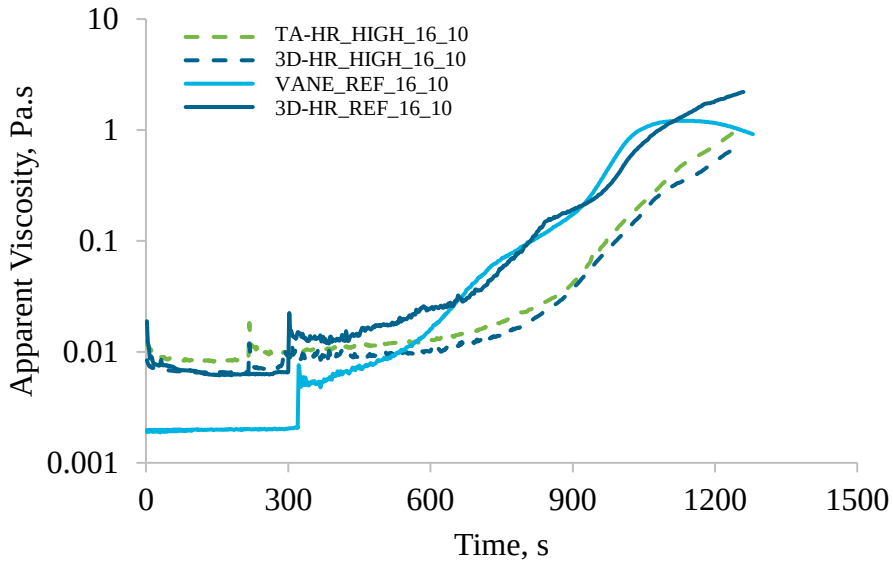

Figure 3. Viscosity-time profiles for samples with 10 minute mixing time and 16. rad.s^{-1} agitator speed

Firstly, examining the vane geometry at T=REF, the system reached a peak viscosity before the end of the process and had started to plateau. However, for the 3D-HR, the viscosity of the system is still increasing at the end of the processing time and has not stabilised, resulting in inhomogeneous final samples (Figure 4). The same result is seen at T=HIGH. The viscosity profiles for the TA-HR and 3D-HR are very similar to each other, suggesting a similar mixing profile, but again there is a failure to achieve a peak viscosity value resulting in inhomogeneous samples. The failure to achieve homogeneity could be related to the energy input to the system. For the vane geometry, the energy input to the peak was 1.24 J/g, and the total energy input 1.95 J/g. For the 3D-HR, the total energy input is 0.71 J/g at T=REF and 0.2 J/g at T=HIGH, and for TA-HR, 0.18 J/g, which are all considerably lower. Whilst the energy input is an important factor, it is known from the previous discussion of sample TA-HR_REF_16_30 (*cf., 3.2*) that it cannot

be used to quantify mixing efficiency in these geometries, as the TA-HR is capable of producing similar viscosity profiles and homogenous samples with lower energy inputs than the other investigated geometries.

The effect of temperature can be seen by the differences in the 3D-HR samples prepared at T=REF and T=HIGH. The higher processing temperature demonstrates apparent viscosity as a function of time (Figure 3). It is difficult to decouple the temperature effects on the viscosity of the continuous phase vs. the differences in LGN microstructure that are formed. Typically, differences in yield stress of the final sample would give an indication of differences in microstructure formation, however as both samples were inhomogeneous, it is difficult to make direct comparisons. Examples of homogeneity of the samples listed in Table 1 are provided in Figure 4 using the methodology outlined in section 2.4.

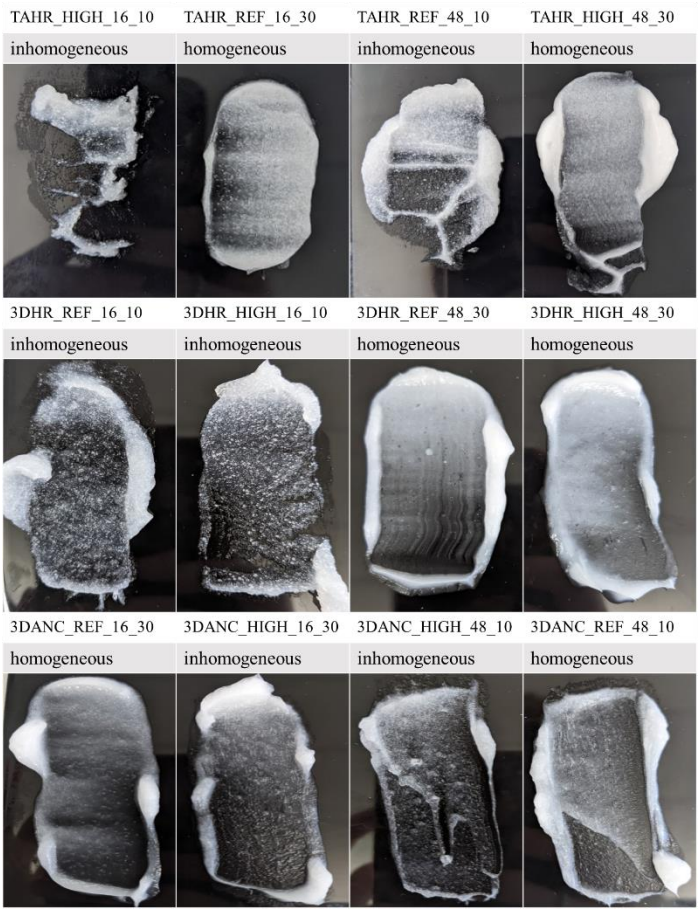

Figure 4. Images of samples detailed in Table 1 showing the degree of homogeneity, where each sample is categorised as homogenous or inhomogeneous based on number of particulates observed

There was a clear effect of mixing time on the homogeneity of the samples that were prepared, whereby all samples that were produced with a mixing time of 30 min were classified as homogeneous, in contrast to samples with a mixing time of 10 min of which 83.33% were categorised as inhomogeneous, regardless of investigated mixing geometry and processing temperature (Figure 4). This behaviour was ascribed to insufficient time being provided to achieve adequate mixing of the system and achievement of a peak viscosity before cooling, as previously discussed (Figure 3). Excluding the yield stress values for the inhomogeneous samples, mixing time also had a significant effect on the yield stress of the final samples (p = 0.0058), where the mean yield stress was higher for the samples produced with a 10 minute mixing time (149 Pa) than the 30 minute mixing time (114 Pa).

3.3 Effect of agitator speed on LGN formation

When the agitator speed was increased from 16 rad s^{-1} to 48 rad s^{-1}, more power was imparted to the system. Three samples were prepared at 48 rad s^{-1} and 10 min mixing time (Table 1), shown in Figure 5.

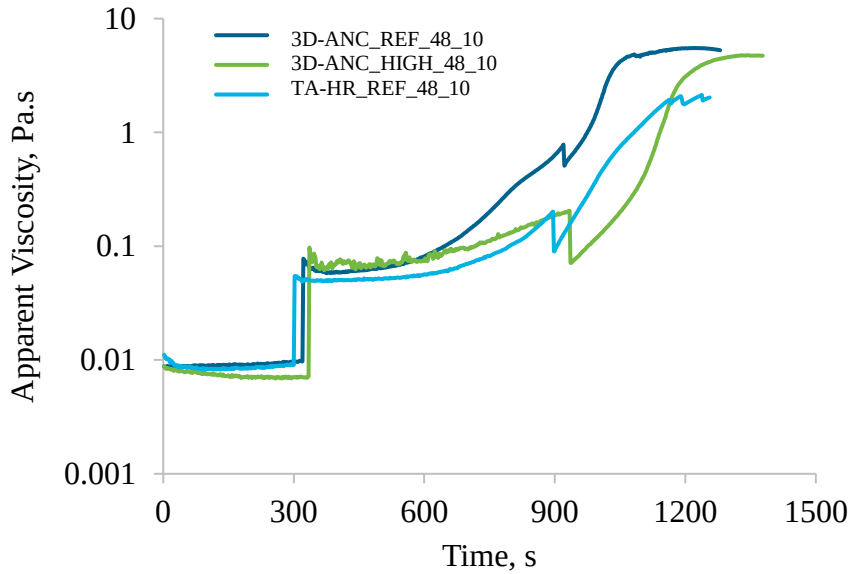

Figure 5. Viscosity-time profiles of samples prepared with 10 min mixing time and 48 rad.s^{-1} agitator speed (3D-ANC_REF_48_10, 3D-ANC_HIGH_48_10, TA-HR_REF_48_10)

For sample 3D-ANC_HIGH_48_10 and TA-HR_REF_48_10, the viscosity has not achieved a plateau by the end of the process, and the resulting LGN samples are inhomogeneous (*cf.*,Figure 4). However, for 3D-ANC_REF_48_10, the peak viscosity occurs before the end of the 10 min processing time, resulting in a homogeneous sample (*cf.*, Figure 4). The energy input to the peak viscosity for 3D-ANC_REF_48_10 was 1.33 J/g, and the sample possessed a final yield stress of 141 Pa (the second highest yield stress for the homogeneous samples). This supports the hypothesis in [5] that a reduced processing time increases the final yield stress of the sample (vane yield stress at same conditions = 139 Pa). Due to the nature of the fractional factorial design of experiments, data for the 3D-ANC at lower processing speeds and 10-minute mixing time was not conducted. At other processing conditions, the 3D-ANC has outperformed the 3D-HR, however it is thought that based on the results for the 3D-HR, which possess a similar shear rate constant (Table 2), that the mixing would not be sufficient at 16 rad s^{-1}, 10 mins to produce a homogeneous sample (Figure 4).

3.4 Effect of processing temperature on LGN formation

Viscosity profiles for the vane and 3D-ANC at two different temperatures (T=REF and T=HIGH) are shown in Figure 6, where the mixing time and agitator speed were the same for each trial, 30 min and 16 rad s^{-1}, respectively. Distinct differences were demonstrated on the rate of viscosity increase during the process due to the dual effect of temperature and mixer type (vane and the anchor geometry).

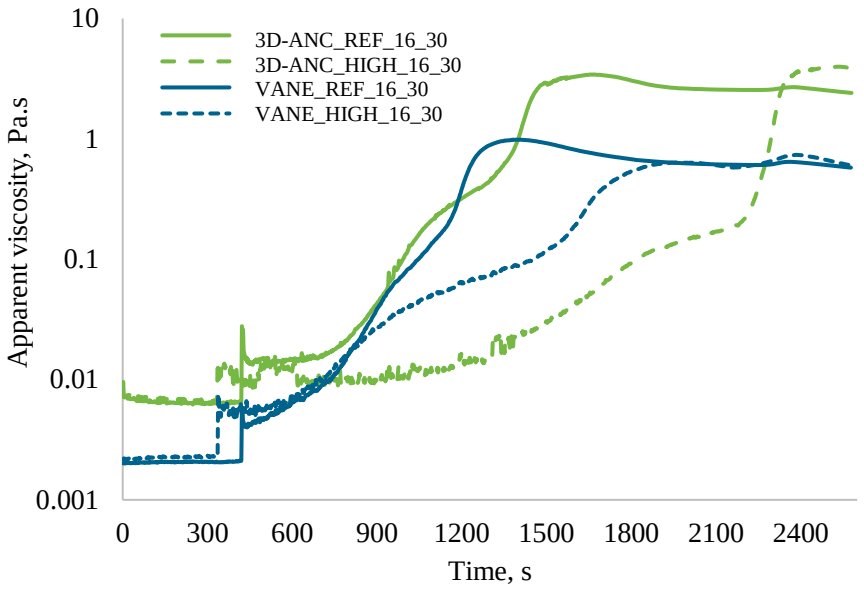

Figure 6. Viscosity-time profiles for samples prepared at different temperatures using the vane and 3D-ANC (Table 1)

For the vane geometry, structure formation occurred at a faster rate when the temperature was at T=REF, however ultimately the final viscosity of the samples was similar for both investigated temperatures (Figure 6). This was reflected in the final characteristics of the sample, where the yield stresses were not significantly different ($p > 0.05$; T=REF = 108 ± 3 Pa; T=HIGH = 104 ± 5 Pa). A comparison between the 3D-ANC and vane at T=REF have already been discussed (*cf.,3.1)*; whilst the apparent viscosity appeared higher for 3D-ANC, the samples had similar final yield stress values, suggesting that this is due to the lower shear rate constant for the 3D-ANC compared to the vane, and the peak viscosity for the 3D-ANC was achieved later, suggesting better mixing in the vane system.

Interesting behaviour was seen for the 3D-ANC at T=HIGH, which did not have repeatable viscosity profiles. In the sample shown here, initially the apparent viscosity was lower for the 3D-ANC in comparison to the vane, and there were fluctuations in the data until the process achieved the cooling stage (*ca.* 2,100s). At this point, the viscosity of the system drastically increased, and the final apparent viscosity was higher than for the sample prepared at T=REF. This correlated with the yield stress of the final product, which was significantly higher for 3D-

ANC_HIGH_16_30 (153 Pa s) than the VANE_HIGH_16_30 (104 ± 5 Pa) and 3D-ANC_REF_16_30 (111 Pa). However, in another repeat of these conditions (data not shown here), the viscosity did not increase at ~2100s, and stayed within the same order of magnitude. This produced a sample which was not homogeneous and on visual inspection, a large lump of fats had collected around the central shaft of the agitator. Perhaps the lower viscosity of the system resulted in a tangentially or radially dominant mixing regime which meant the fats were not able to be incorporated properly [13].

3.5 Effect of processing variables on final product yield stress of LGNs

Figure 7a shows the range of yield stress measurements for the samples collected for each geometry type for all process conditions, including samples which were not homogeneous (Figure 4). The differences in means of the yield stresses of the samples produced using each geometry were not significantly different (p = 0.645 using ANOVA). However, this does not preclude the fact that the geometries perform differently at different process conditions, evidenced by the range of yield stresses, and the fact that the means have been compared across different process conditions.

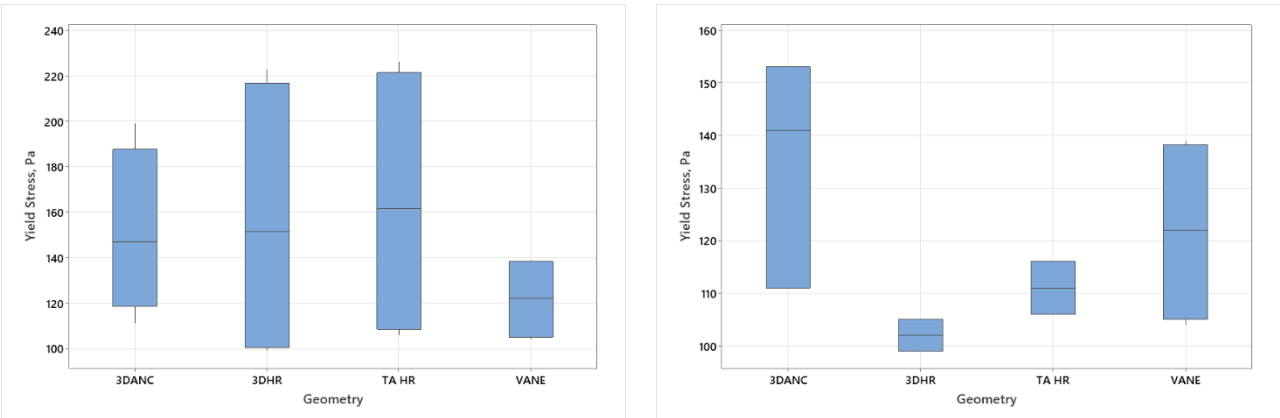

Figure 7. Box plot of yield stress measurements of final product samples by geometry type ((a) including heterogeneous samples; (b) excluding heterogeneous samples

It should be noted that the majority of the high yield stress measurements were for samples which were inhomogeneous, and the high value was likely due to the fact that the LGN microstructure had not been fully formed. The presence of unincorporated solid fatty alcohol and

surfactant in the sample causes jamming in the rheometer and affects the measurement (Figure 4). Examining examples of amplitude sweeps, the difference between the loss modulus (*G″*) and

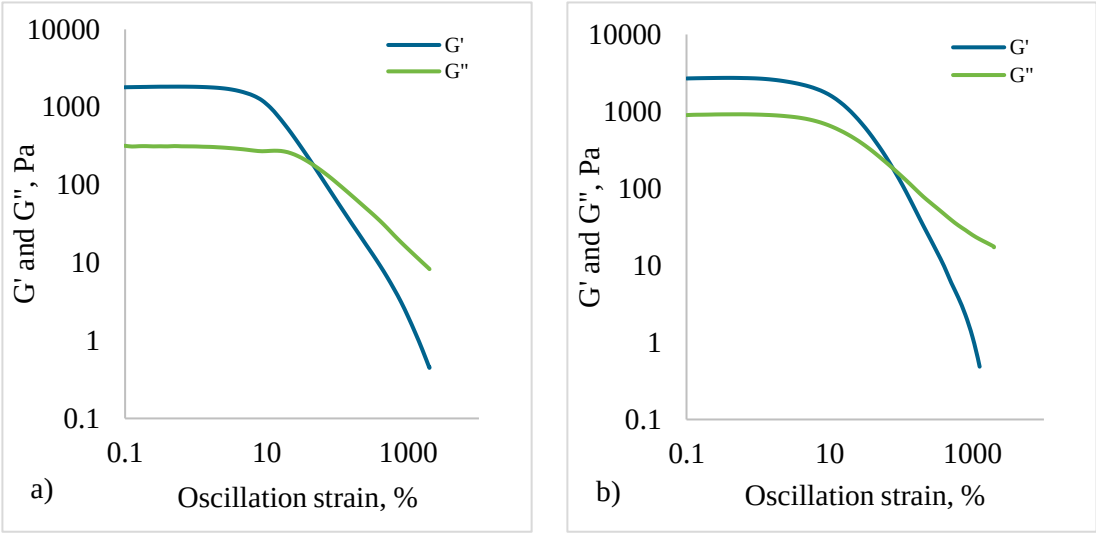

Figure 8. a) Oscillation amplitude sweep for 3D-HR_REF_16_30 b) Oscillation amplitude sweep for 3D-HR_REF_16_10

storage modulus (*G′*) were smaller for samples that were processed with a 10 min mixing time, which suggests less viscoelasticity (Figure 8b). Conversely, for a sample which was processed with a 30 min mixing time, it exhibited the characteristic overshoot in the loss modulus prior to the cross over-point, which depicts the breakdown of a cross-linked gel structure, similar to that observed for LGNs (Figure 8a) [13].

Further analysis of the effect of geometry on yield stress was conducted, excluding the inhomogeneous samples (Figure 7b) comparing the mean yield stress for each geometry when samples are prepared at a range of conditions, the 3D-ANC is highest (137 Pa), followed by the vane (121.75 Pa), TA-HR (111 Pa), 3D-HR (104 Pa). This could be due to effects of the fractional factorial design, where optimal processing conditions have been randomly selected for certain geometries; but does suggest that generally the 3D-ANC is capable of producing samples with higher yield stresses. Using a student's t-test, it was also shown that the yield stresses were significantly different for 3D-ANC and 3D-HR ($p = 0.0392$).

4 Conclusions

This study monitored the structure formation of lamellar gel liquids in-situ using a rheometer with different mixing rheometer geometries: conventional four-bladed vane, commercially available helical rotor (TA-HR) and two bespoke geometries, 3D printed in titanium, a helical ribbon (3D-HR) and an anchor scraper (3D-ANC). Viscosity-time profiles as a function of process variables and yield stress measurements on manufactured samples as per design of experiments were used to assess the impact of changing geometry. The results suggested that there were differences in the mixing capability of each investigated geometry, particularly for short processing times. For the 10 min samples prepared at 16 rad s^{-1}, the 3D-HR and TA-HR were not capable of producing a homogeneous sample, whereas the vane was (3D-ANC was not tested at these conditions due to the nature of the fractional factorial design of experiments). This was likely due to differences in energy input into the system which was related to the shape, mass, and surface area of the rheometer geometry. The two samples with the highest yield stresses (which were homogeneous) were both produced using the 3D-ANC, yet at different process conditions (3D-ANC_HIGH_16_30 = 153 Pa; 3D-ANC_REF_48_10 = 141 Pa). The energy input to the peak viscosity for these samples was 1.152 J/g and 1.327 J/g, respectively. Hence, the longer mixing time at a lower speed was more energy efficient for this geometry. Overall, the industrially relevant geometries did not follow the same trends as the vane geometry, highlighting the importance of investigating how the mixing characteristics are affected by the interplay between geometry and processing conditions. The next steps for this work are to utilise the information collected to generate information around the power requirements of each type of geometry, and how this could be optimised to produce an LGN which is homogenous, achieves peak viscosity efficiently and possessing a high yield stress, with the lowest possible energy consumption. Power numbers for the geometries will be generated in order to determine the usefulness of this technique in scale-up. Overall, the application of industrially relevant geometries has provided a better insight into how the combination of processing conditions and geometry can result in different mixing characteristics within the vessel, and the resulting impact on the product characteristics.

Acknowledgments

The authors would like to acknowledge Darren Lamb, Emily Robinson, Serena Todd, and Adam Rowatt from University of Strathclyde for their support designing the bespoke mixing elements, and Alan Magowan from Laser Proto Europe Ltd for providing 3D printing services. Additionally, the authors acknowledge financial support received from the Centre for Doctoral Training in Formulation Engineering (EPSRC grant no.EP/S023070.1)

Conflict of Interest Statement

The authors declare that they have no known competing financial interests or personal relationships that could have appeared to influence the work reported in this paper.

References

[1] Statista Research Department, "Global value of the cosmetics market 2018-2025," Statista, 2 February 2022. [Online]. Available: https://www.statista.com/statistics/585522/global-value-cosmetics-market/. [Accessed 5 June 2022].

[2] J. E. Hobbs, "Food supply chains during the COVID-19 pandemic," *Canadian Journal of Agricultural Economics,* vol. 68, no. 2, pp. 171-176, 2020.

[3] C. Jira and M. W. Toffel, "Engaging Supply Chains in Climate Change," *Manufacturing & Service Operations Management,* vol. 15, no. 4, pp. 1-19, 2013.

[4] C. Wibowo and K. M. Ng, "Product-Centered Processing: Manufacture of Chemical-Based Consumer Products," *AIChE Journal,* vol. 48, no. 6, pp. 1212-1230, 2002.

[5] G. Cunningham, F. Alberini, M. Simmons and J. O'Sullivan, "Understanding the effects of processing conditions of the formation of lamellar gel networks," *Chemical Engineering Science,* 2021.

[6] C. E. Owens, A. J. Hart and G. H. McKinley, "Improved rheometry of yield stress fluids using bespoke fractal 3D printed vanes," *Journal of Rheology,* vol. 64, no. 643, 2020.

[7] P. Cullen, C. O'Donnell and M. Houska, "Rotational Rheometry Using Complex Geometries - A Review," *Journal of Texture Studies,* vol. 34, pp. 1-20, 2003.

[8] A. Franck, "Non-standard geometries for rheological characterization of complex fluids".

[9] A. Ait-Kadi, P. Marchale, L. Choplin, A. Chrissemant and M. Bousmina, "Quantative Analysis of Mixer-Type Rheometers using the Couette Analogy," *The Canadian Journal of Chemical Engineering,* vol. 80, 2002.

[10] A. Davies and S. Amin, "Microstructure design of CTAC:FA and BTAC:FA lamellar gels for optimized rheological performance utilizing automated formulation platform," *International Journal of Cosmetic Science,* vol. 42, pp. 259-269, 2020.

[11] A. Datta, V. S. Tanmay, G. X. Tan, G. W. Reynolds, S. N. Jamadagni and R. G. Larson, “Characterizing the rheology, slip, and velocity profiles of lamellar gel networks,” *Journal of Rheology*, vol. 64, 2020.

[12] O. Mihailova, T. Mothersdale, T. Rodgers, Z. Ren, S. Watson, V. Lister and A. Kowalski, “Optimisation of mixing performance of helical ribbon mixers for high throughput applications using computational fluid dynamics,” *Chemical Engineering Research and Design*, vol. 132, pp. 942-953, 2018.

[13] M. Youssry, L. Coppola, I. Nicotera and C. Morán, “Swollen and collapsed lyotropic lamellar rheology,” *Journal of Colloid and Interface Science* , vol. 321, pp. 459-467, 2008.